

# Loss of $\alpha$ -Catenin Decreases the Strength of Single E-cadherin Bonds between Human Cancer Cells\*

Received for publication, March 30, 2009, and in revised form, May 13, 2009. Published, JBC Papers in Press, May 19, 2009, DOI 10.1074/jbc.M109.000661

Saumendra Bajpai<sup>‡</sup>, Yunfeng Feng<sup>§</sup>, Ranjini Krishnamurthy<sup>‡</sup>, Gregory D. Longmore<sup>§</sup>, and Denis Wirtz<sup>‡¶1</sup>

From the <sup>‡</sup>Department of Chemical and Biomolecular Engineering, The Johns Hopkins University, Baltimore, Maryland 21218, the

<sup>§</sup>Departments of Physiology and Cell Biology, Washington University School of Medicine, St. Louis, Missouri 63110, and the

<sup>¶</sup>Department of Oncology, Johns Hopkins Kimmel Cancer Center, Johns Hopkins School of Medicine, Baltimore, Maryland 21231

The progression of several human cancers correlates with the loss of cytoplasmic protein  $\alpha$ -catenin from E-cadherin-rich intercellular junctions and loss of adhesion. However, the potential role of  $\alpha$ -catenin in directly modulating the adhesive function of individual E-cadherin molecules in human cancer is unknown. Here we use single-molecule force spectroscopy to probe the tensile strength, unstressed bond lifetime, and interaction energy between E-cadherins expressed on the surface of live human parental breast cancer cells lacking  $\alpha$ -catenin and these cells where  $\alpha$ -catenin is re-expressed. We find that the tensile strength and the lifetime of single E-cadherin/E-cadherin bonds between parental cells are significantly lower over a wide range of loading rates. Statistical analysis of the force displacement spectra reveals that single cadherin bonds between cancer cells feature an exceedingly low energy barrier against tensile forces and low molecular stiffness. Disassembly of filamentous actin using latrunculin B has no significant effect on the strength of single intercellular E-cadherin bonds. The absence of  $\alpha$ -catenin causes a dominant negative effect on both global cell-cell adhesion and single E-cadherin bond strength. These results suggest that the loss of  $\alpha$ -catenin alone drastically reduces the adhesive force between individual cadherin pairs on adjoining cells, explain the global loss of cell adhesion in human breast cancer cells, and show that the forced expression of  $\alpha$ -catenin in cancer cells can restore both higher intercellular avidity and intercellular E-cadherin bond strength.

The reduction of intercellular adhesion in a solid tumor is a critical step in the progression of tumor cells to metastasis (1). How normal cells lose their ability to form strong adhesions within a tissue is not well understood (2, 3). The loss of adhesion between adjoining epithelial cells and the ensuing onset of metastasis occur through an epithelial-to-mesenchymal transition that often correlates with the loss of cytoplasmic protein  $\alpha$ -catenin and a poor prognosis in a wide range of cancers, including breast (4), esophageal (5), gastric (6, 7), cervical (8), and colorectal cancer (9). In normal epithelial tissues,  $\alpha$ -catenin

localizes to junctions that organize at the interface between adjacent epithelial cells through clustering of cell surface adhesion transmembrane molecule cadherin and its association to the cytoskeleton (10, 11). On the extracellular side, structural studies suggest that cadherin molecules form molecular pairs that interact with cadherin pairs on an adjacent cell through their distal  $\text{Ca}^{2+}$ -binding domains (12). On the intracellular side, cadherin pairs are connected to the cytoskeleton network through specific linker proteins. Until recently it was believed that one critical linker protein between the cytoplasmic domain of cadherin and the actin cytoskeleton was  $\alpha$ -catenin, because it can both bind filamentous actin (F-actin) and E-cadherin through  $\beta$ -catenin (13, 14). However, a recent study indicates that  $\alpha$ -catenin can either bind the E-cadherin- $\beta$ -catenin complex as monomer or cross-link actin filaments as homodimer but cannot bind both E-cadherin- $\beta$ -catenin and F-actin simultaneously (15). Therefore, whether the loss of  $\alpha$ -catenin plays a direct role in the loss of adhesion in human cancer cells is unclear.

Our recent data using engineered Chinese hamster ovarian cells suggest that  $\alpha$ -catenin mediates the rapid strengthening of individual intercellular E-cadherin/E-cadherin bonds following initial molecular recognition between cells bearing E-cadherin molecules (16). Furthermore,  $\alpha$ -catenin mediates the formation of additional E-cadherin/E-cadherin bonds once a first bond is formed between adjoining cells to form a nascent intercellular junction (16). Here we hypothesize that the loss of cytoplasmic protein  $\alpha$ -catenin in human cancer cells greatly affects the ability of E-cadherin molecules on the surface of these cells to form firm adhesion by reducing the strength of individual intercellular E-cadherin/E-cadherin bonds.

Our strategy is to compare parental breast cancer cells that lack  $\alpha$ -catenin (MDA-MB-468 cells; denoted here MDA468) with these cells when  $\alpha$ -catenin is introduced and exploit high resolution live cell single-molecule force spectroscopy (17) to probe the strength of individual E-cadherin/E-cadherin bonds between adjacent cells (18). The cells are juxtaposed for a controlled time of contact, the probability of successful interactions is subsequently measured, and the mechanical properties (tensile strength, molecular stiffness, and reactive compliance) and biochemical properties (interaction energy, dissociation rate, and bond lifetime) of single intercellular E-cadherin/E-cadherin bonds are analyzed.

Our main hypothesis cannot be readily tested using purified proteins. Our ability to measure molecular interactions between live cells (17) rather than recombinant proteins

\* This work was supported, in whole or in part, by National Institutes of Health Grants GM080673 (to G. D. L.) and CA137891 (to D. W.). This work was also supported by Grant-in-aid 0855319E from the American Heart Association (to D. W.).

<sup>1</sup> To whom correspondence should be addressed: Depts. of Chemical and Biomolecular Engineering, The Johns Hopkins University, 3400 N. Charles St., Baltimore, MD 21218. Fax: 410-516-5510; E-mail: wirtz@jhu.edu.

ensures that the proper orientation of cadherin on the cell surfaces and its post-translational modifications are physiological. Moreover, using living cells ensures that the cytoplasmic domain of transmembrane receptors (here human E-cadherin) can interact with cytoplasmic proteins (in particular  $\beta$ -catenin and  $\alpha$ -catenin), thereby allowing cell signaling pathways that can influence cell adhesion to function normally.

## EXPERIMENTAL PROCEDURES

**Cell Culture and Western Blot Analysis**—MDA-MB-468 is a human breast carcinoma cell line derived from a 51-year-old black female (19). MDA468 cells show no measurable expression of  $\alpha$ -catenin (see Fig. 1). MDA468 cells where  $\alpha$ -catenin was stably transfected are those described in Ref. 20. Parental MDA468 and MDA468 cells engineered to stably express  $\alpha$ -catenin were cultured in Dulbecco's modified Eagle's medium (Invitrogen), supplemented with 10% bovine calf serum (ATCC, Manassas, VA) and 1% penicillin/streptomycin. These cells were cultured in DMEM-10 (Dulbecco's modified Eagle's medium supplemented with 10% fetal bovine serum and penicillin/streptomycin). A 70% confluent T-25 flask, incubated at 37 °C and 5% CO<sub>2</sub>, was harvested for loading cells on molecular force probe cantilevers, as well as plated on a bottom culture dish. The cells were washed in Hanks' balanced salt solution (Invitrogen) and incubated with 1 ml of trypsin-EDTA (Invitrogen) for 5 min, resuspended in 5 ml of cell culture medium. The cells were then plated for normal passing into a new T-25 flask, mixing 1 ml of resuspended cells in 4 ml of fresh culture medium. Prior to molecular force probe measurements, the cells were passed into a 50-mm Corning dish and incubated overnight. For all procedures that had to be conducted outside of the incubator, the culture medium was supplemented with 2% HEPES (Invitrogen) to control pH.

For the preparation of cell lysates, subconfluent cultures of the cells in p100 cell culture dishes were washed twice with ice-cold 1× phosphate-buffered saline, 300  $\mu$ l of ice-cold lysis buffer (50 mM Tris-HCl, pH 7.6, 150 mM NaCl, 1 mM EDTA, 5 mM NaF, 1 mM sodium orthovanadate, 0.5% Nonidet P-40, 0.25% sodium deoxycholate, 1 mM dithiothreitol, and protease mixture freshly added) were added to the plates and collected with cell lifter, vortexed in Eppendoff tubes, and maintained on ice for 10 min with vortex every 2 min to obtain the cell lysates. Protein concentrations were determined using a protein assay reagent (Cytoskeleton Inc., Denver, CO). For Western blot analysis, 20  $\mu$ g of cell lysate were mixed equal volume of 2× SDS protein loading buffer, boiled, and loaded to each lane. After electrophoresis, the proteins were transferred to polyvinylidene difluoride membrane, and each panel was immunoblotted with antibodies as described in the figure.

**Surface Expression of E-cadherin**—Standard flow cytometry was used to quantify possible changes in cell surface expression of E-cadherin (see Fig. 2c). Briefly, single cells were suspended in staining buffer (phosphate-buffered saline, 2% fetal calf serum) and incubated with primary HECD1 anti-human E-cadherin monoclonal antibody (Zymed Lab, San Francisco, CA) for 30 min on ice. The cells were washed twice in staining buffer and incubated with goat anti-mouse Alexa Fluor secondary antibody for 30 min in the dark and washed thoroughly. The

stained cells were immediately used for measurements of cell surface expression using flow cytometry. IgG1 type anti-mouse antibody was used as isotype control (Sigma).

Immunofluorescence microscopy confirmed these results (Fig. 2b). For immunofluorescence microscopy studies, the cells were plated on glass-bottomed dishes and fixed according to the standard protocol. Mouse anti-human  $\alpha$ -catenin monoclonal antibody (Novus Biologicals, Littleton, CO) was used for staining the fixed samples for  $\alpha$ -catenin.

**Preparation of AFM<sup>2</sup> Cantilevers**—The softest available AFM cantilevers, with nominal force constant around 10 pN/nm, were used (model MLCT-AUHW; Veeco Instruments, Plainview, NY). Cantilevers were cleaned thoroughly with 70% EtOH, 10% HCl solution, ultrapure water, and 95% EtOH for 1 min each, followed by 5 min washing with acetone. The cleaned cantilever was immediately used for loading cells or incubated at room temperature in phosphate-buffered saline for later use.

**Loading Live Cells on AFM Cantilever Tips**—A flame-blown borosilicate microneedle (Sutter Instruments, Novato, CA) was used to deposit four or five cells on the tip of the AFM cantilever. The procedure was carried out using a temperature-controlled TE-2000 Nikon microscope, using a 10× Plan Fluor objective (N.A. 0.3) and an Eppendorf Transjector 5246 (Brinkmann Instruments, Riverview, FL). pH in the medium was maintained using 2% HEPES. Cells deposited on the cantilevers were allowed to spread overnight.

**Single-molecule Force Spectroscopy**—Single-molecule force spectroscopic measurements were made using a piconewton sensitive molecular force probe (MFP-1D; Asylum Research, Santa Barbara, CA). The cantilever carrying cells was brought in contact for 1 ms with a bottom layer of cells (plated on a 50-mm dish) and retracted. Prior to single-molecule force spectroscopic measurements, the 50-mm Corning dish with plated cells was washed thoroughly with Hanks' balanced salt solution (Invitrogen) and was filled with 5 ml of serum-free medium supplemented with 2% HEPES, preheated to 37 °C. The rupture of intercellular bonds could be visualized as sharp peaks in the force-distance curves (see Fig. 1). The cantilevers were calibrated for their rigidity and optical lever sensitivity. The method of thermal resonance was used for calibrating the force constant, whereas the inverse of optical sensitivity was obtained by lowering the cantilever on a hard surface by a known distance and measuring the corresponding voltage signal (17, 18). Because calibration of the cantilever involves large impingement forces leading to rupture of cell and/or detachment of the cell from the cantilever, calibration was done at the end of the experiments, as per the manufacturers' protocol. Depending on the calibration, the height of the peak yielded the force required to break a bond.

**Single-molecule Data Acquisition and Analysis**—Using the built-in digital camera in the molecular force probe body, the cantilever was lowered at a specified velocity. Approximately 30 force-distance curves for a given retraction velocity were collected per cell. The cantilever was then moved to another location in the dish to ensure proper sampling. To move the canti-

<sup>2</sup> The abbreviation used is: AFM; atomic force microscope.

## $\alpha$ -Catenin Enhances E-cadherin Adhesion

lever to a new location on the plated cells, the cantilever was manually raised, and the plated cells were shifted using side screws. Data collection and analysis were conducted using Igor-Pro 4.09 software (Wavemetrics, Inc., Lake Oswego, OR). The loading rate applied on an intercellular bond was calculated as the product of the retraction velocity and the slope of the force curve immediately before bond rupture (see Fig. 1). Only the last rupture in a force-distance curve was analyzed, because the strength of the last bond could be modulated by the presence of earlier bonds. The noise in measurements was  $<10$  pN; subsequently, all ruptures smaller than the noise were disregarded. The measured ruptures were binned, using 5-pN-wide bins. The force distribution for a given velocity was fitted using Hummer and Szabo's model, and corresponding fitting parameters were obtained by the random search method (21). To evaluate the loading rate dependence of bond strengths, 100 pN/s wide bins were used below 1000 pN/s, and 1000-pN/s bins were used between 1000 pN/s and 10,000 pN/s.

**Global Intercellular Adhesion Assay**—A 96-well plate was used to grow cells to confluence. It was ensured that the entire well was covered with a monolayer of cells. Just prior to the assay, each well was washed thoroughly to ensure that all rounded/floating cells were removed. Cells tagged with carboxyfluorescein diacetate succinimidyl ester (Invitrogen) as per manufacturer's protocol were introduced into each well at  $10^4$  cells/well. The tagged cells were allowed to adhere to the monolayer of cells in each well for 1 h, followed by inversion of the 96-well plate for 6 min, using a static adhesion chamber (Glyco-Tech, Gaithersburg, MD). The cells that fell off were allowed to settle down at the base of the inverted chamber. The base plate was then removed. Pre- and post-inversion readings of the fluorescence intensity in each well was measured using a fluorescence plate reader. The ratio of the fluorescence reading in each well after inversion to that before inversion related to the degree of cell-cell adhesion; the higher the ratio, the greater the extent of cell-cell adhesion.

**Specificity of Single-molecule Force Spectroscopy Measurements**—For E-cadherin function-blocking controls, plated cells were treated with HEC1 anti-human E-cadherin monoclonal antibody (Zymed Lab) at a concentration of 200  $\mu$ g/ml for 30 min at 37 °C and 5% CO<sub>2</sub>. Postincubation, 4 ml of serum-free medium was added, and the cells were immediately used for measurements.

## RESULTS AND DISCUSSION

The main hypothesis of this study is that the loss of  $\alpha$ -catenin in certain human breast cancer cells causes a failure of E-cadherin molecules on the surface of these cells to form strong individual intercellular bonds. Using live cell single-molecule force spectroscopy, we probed the biomechanical and biochemical properties of individual cadherin bonds formed between two juxtaposed living parental MDA468 breast cancer cells, which lack  $\alpha$ -catenin, or MDA468 cells where  $\alpha$ -catenin is expressed (Fig. 1a).

Single cells were delicately placed and allowed to spread on the surface of soft triangular cantilevers using weakly adhesive microneedles under a light microscope (Fig. 1b). The rigidity of the cantilever (5–20 pN/nm) was measured prior to each exper-

iment to measure adhesion forces between cadherin molecules forming individual bonds on opposing cells with piconewton force resolution. The cell on the cantilever was gently brought into contact with a cell on a bottom culture dish (Fig. 1b). The repeated approach and retraction of the top cell to and from the bottom cell set at a controlled retraction velocity (either 5 or 30  $\mu$ m/s) produced force displacement spectra, which were recorded with high temporal resolution (Fig. 1c). The presence of an abrupt drop in the spectrum indicated the rupture of an intercellular bond between the top and bottom cells (Fig. 1c, arrows). Fig. 1c shows typical features exhibited by force displacement curves, including the rupture of no intercellular bond, one bond, and more than one bond during the retraction of the top cell from the bottom cell. The height of the force drop is the tensile strength of the bond that was formed upon cell contact, and the product of the retraction velocity by the slope of the force spectrum just prior to bond rupture is the loading rate applied to that bond (Fig. 1c).

The time of contact (typically 1 ms) and impingement force (200–500 pN) were adjusted to allow for only very few successful binding interactions to occur between E-cadherin molecules on the surfaces of adjacent cells. These conditions allowed us to target  $\sim 28\%$  of force-distance spectra displaying at least one bond rupture event (Fig. 1d). In these conditions, the probabilities of forming a single adhesive bond, two bonds, and three bonds upon cell-cell contact are 85, 12, and  $<2\%$ , respectively (22).

MDA468 cancer cells express a wide range of adhesion molecules on their surface, including integrin, epithelial cell adhesion molecule (C-CAM), and E-cadherin. To ensure that our measurements of intercellular adhesion are mainly due to Ca<sup>2+</sup>-activated E-cadherin, cells were either treated with chelating molecule EDTA or treated with a specific anti-E-cadherin function-blocking monoclonal antibody. In both cases, the probability of interactions between cancer cells was reduced to background levels (Fig. 1d). These levels of interactions are comparable with those between a bare cantilever (no cell present) and cells on the bottom dish (data not shown). These results indicate that our single-molecule force spectroscopy measurements are specific and that binding interactions between individual cancer cells are dominated by homotypic E-cadherin interactions.

We developed a cell line stably expressing  $\alpha$ -catenin based on the parental MDA468 cell line (Fig. 2). Notably, immunoprecipitation and Western blot analysis (Fig. 2a), immunofluorescence microscopy (Fig. 2b), and flow cytometry (Fig. 2c) suggested that MDA468 parental cells and  $\alpha$ -catenin-positive cells showed the same levels of expression of E-cadherin. A simple global cell adhesion assay (see "Experimental Procedures") showed that global intercellular adhesion (as opposed to single-molecule level adhesion) was significantly increased in  $\alpha$ -catenin-expressing MDA468 cells compared with  $\alpha$ -catenin-lacking MDA468 cells (Fig. 1e). Because levels of surface expression of E-cadherin were similar (Fig. 2), this result suggests that the lower cell-cell adhesion for MDA468 cells is caused by the absence of  $\alpha$ -catenin.

We sought to determine whether this loss of global intercellular adhesion was due to an increased adhesion strength of



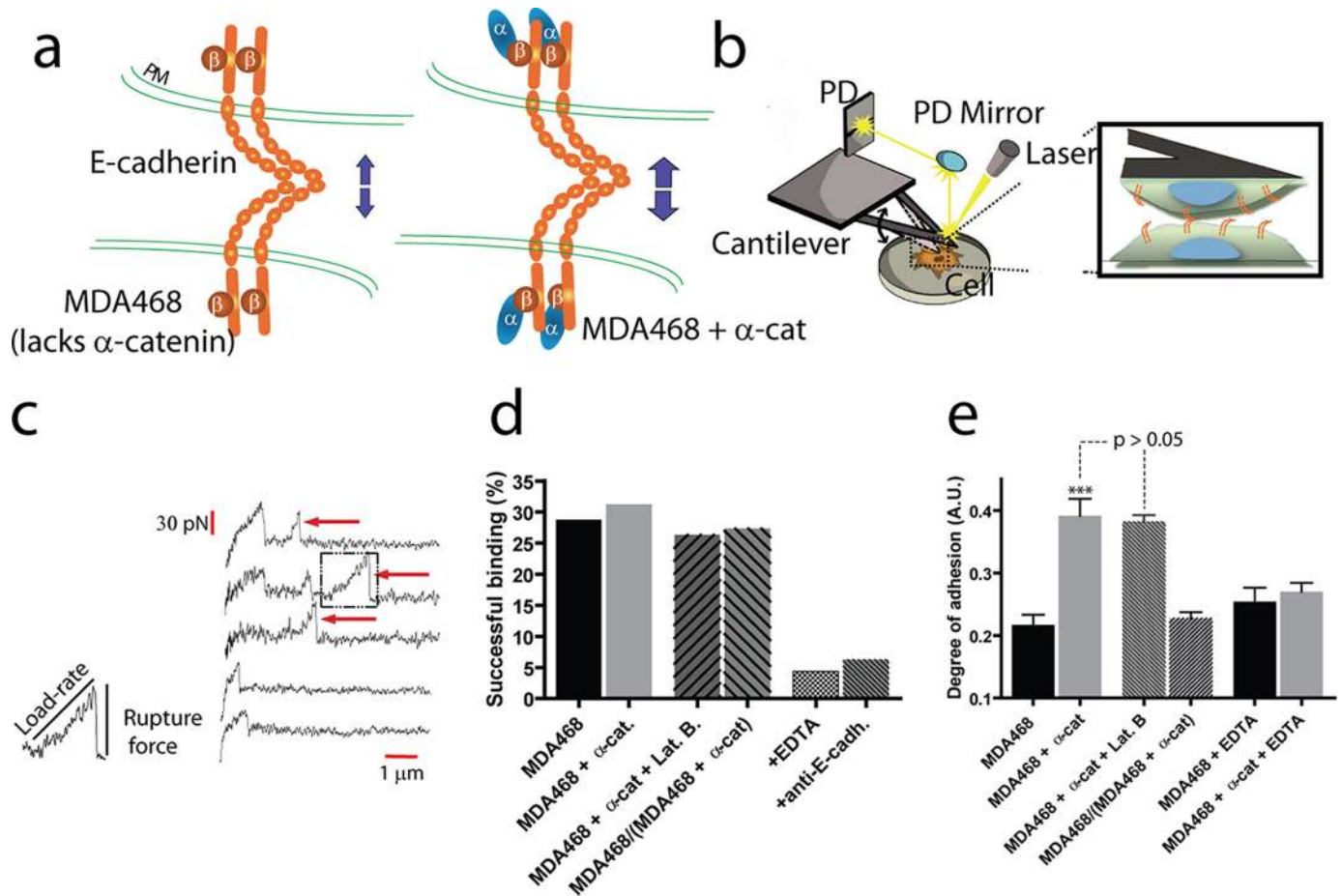


**FIGURE 1. Single-molecule force spectroscopy reveals the micromechanical and biochemical properties of individual E-cadherin/E-cadherin bonds between live human cancer cells.** *a*, schematic of homotypic interactions of E-cadherin (*E-cadh*) pairs on either juxtaposed MDA468 cells that lacked  $\alpha$ -catenin ( $\alpha$ -cat) or juxtaposed MDA468 cells where  $\alpha$ -catenin was expressed. *b*, schematic of the instrument used to probe E-cadherin-mediated interactions between a cell placed on a soft calibrated cantilever and a cell adherent to a bottom culture dish. *Inset*, a bond is formed between cadherin pairs on adjacent cells. *c*, when the cantilever is retracted at a controlled velocity, force displacement spectra are recorded with high force and temporal resolutions. The arrows indicate abrupt drops in force corresponding to the rupture of intercellular cadherin bonds that had been formed upon controlled contact between the two cells. *d*, probability of successful bond formation between parental MDA468 cells (first bar),  $\alpha$ -catenin-expressing MDA468 cells (second bar),  $\alpha$ -catenin-expressing MDA468 cells in the presence of the actin depolymerizing drug latrunculin B (third bar), MDA468 cells and  $\alpha$ -catenin-expressing MDA468 cells (fourth bar), MDA468 cells in the presence of EDTA (fifth bar), and MDA468 cells in the presence of anti-E-cadherin antibody (sixth bar). *e*, global intercellular adhesion between MDA468 cells (first bar),  $\alpha$ -catenin-expressing MDA468 cells (second bar),  $\alpha$ -catenin-expressing MDA468 cells in the presence of latrunculin B (third bar), MDA468 cells and  $\alpha$ -catenin-expressing MDA468 cells (fourth bar), MDA468 cells in the absence of EDTA (fifth bar), and  $\alpha$ -catenin-expressing MDA468 cells in the presence of EDTA (sixth bar).

individual intercellular E-cadherin/E-cadherin bonds. Using single-molecule force spectroscopy (17), we characterized the force required to rupture individual E-cadherin/E-cadherin bonds (also called the tensile strength or de-adhesion force of the bond) as a function of the loading rate on the bonds (Fig. 3*a*). We found that the mean tensile strengths of homotypic E-cadherin/E-cadherin bonds between parental cells and between  $\alpha$ -catenin-expressing cells increased both logarithmically with loading rate. Such a micromechanical response is observed for a wide range of ligand-receptor pairs, including P-selectin-CD44 (23), selectin-PSGL-1 (24), N-cadherin/N-cadherin (18), and VE-cadherin/VE-cadherin bonds (25).

Importantly, the mean tensile strength of E-cadherin/E-cadherin bonds between parental cells was significantly lower than the tensile strength of E-cadherin/E-cadherin bonds between  $\alpha$ -catenin-expressing cells over a wide range of loading rates (Fig. 3, *a* and *b*). Because rupture forces are distributed (see Fig. 5), we also compared the most probable

bond rupture forces at given loading rates and found similar trends (Fig. 3, *b* and *c*) (26). Therefore, forced expression of  $\alpha$ -catenin greatly increases the strength of single E-cadherin adhesion bonds.

From fits of the mean bond strength *versus* loading rate using Bell model analysis (24, 27), we extracted the unstressed dissociation rate,  $k_{\text{off}}^0$  and the reactive compliance,  $x_{\beta}$ , of single E-cadherin/E-cadherin bonds between parental breast cancer cells and E-cadherin/E-cadherin bonds between  $\alpha$ -catenin-expressing cells, respectively (Fig. 4, *a* and *b*). The unstressed dissociation rate describes the rate at which spontaneous unbinding between cadherin molecules on opposing cells occurs; the reactive compliance describes the effective molecule length over which cadherin molecules on opposing cells disengage from each other upon unbinding. We found that the absence of  $\alpha$ -catenin in parental cells caused a significant increase in the unstressed dissociation rate (Fig. 4*b*). Accordingly, the unstressed bond lifetime,  $1/k_{\text{off}}^0$  was increased 7-fold for cells expressing  $\alpha$ -catenin (Fig. 4*c*). These

## $\alpha$ -Catenin Enhances E-cadherin Adhesion

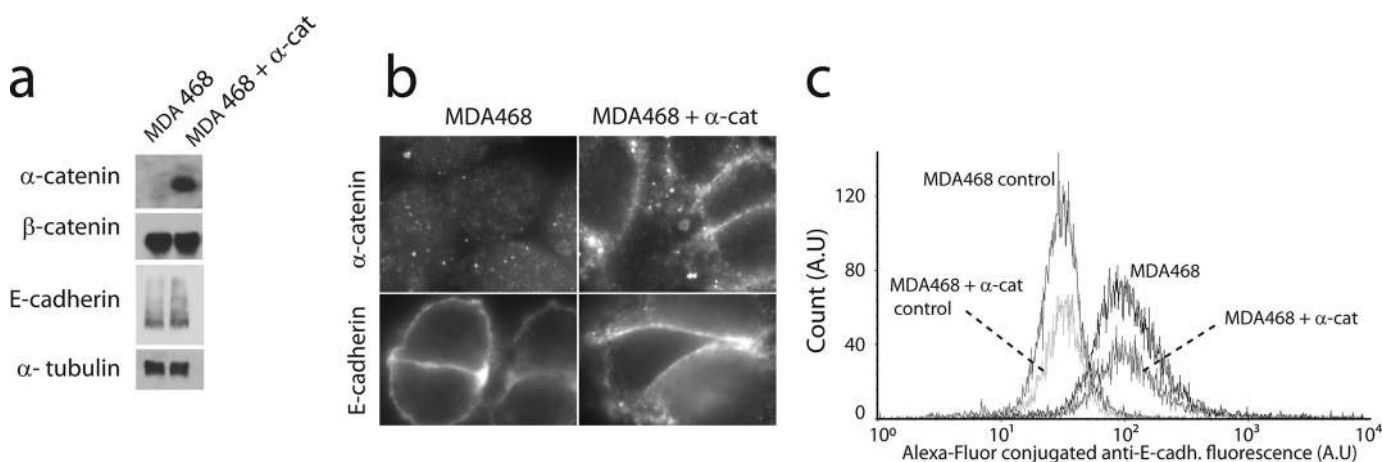


**FIGURE 2. Western blot, immunofluorescence microscopy, and flow cytometry analysis of E-cadherin expression.** *a*, immunoprecipitation and Western blot analysis of expression of E-cadherin,  $\beta$ -catenin, and  $\alpha$ -catenin in MDA468 and  $\alpha$ -catenin-expressing MDA468 cells. *b*, immunofluorescence microscopy of  $\alpha$ -catenin and E-cadherin in parental MDA468 cells and MDA468 cells expressing  $\alpha$ -catenin. *a* and *b* show that parental MDA468 cells lack  $\alpha$ -catenin and that the levels of expression of E-cadherin and  $\beta$ -catenin are not significantly changed by the forced expression of  $\alpha$ -catenin in MDA468 cells. *c*, flow cytometry analysis of the levels of expression of E-cadherin on the surface of MDA468 cells and that of MDA468 cells expressing  $\alpha$ -catenin. The location of maxima as well as the geometric means for the experiments were nearly identical, signifying quantitatively similar surface expression levels of E-cadherin.

results suggest that the loss of  $\alpha$ -catenin in cancer cells resulted in much shorter lived cadherin bonds between cells.

The reactive compliance of individual E-cadherin/E-cadherin bonds was also different: 0.76 nm *versus* 0.51 nm for MDA468 cells and  $\alpha$ -catenin-expressing MDA468 cells, respectively (Fig. 4*d*). A higher reactive compliance indicates E-cadherin/E-cadherin bonds between cancer cells that lack  $\alpha$ -catenin are more prone to rupture than the same cells where  $\alpha$ -catenin is expressed.

We note that bond lifetimes determined by fitting force spectra to Bell's model have values that can be at variance with values obtained by direct measurements of bond lifetimes (28). Although this discrepancy can be attributed to the difference in model systems used (live cell in our case compared with purified proteins), this difference in absolute values does not alter our main conclusions regarding the role played by  $\alpha$ -catenin in cell-cell adhesion.

The forces required to rupture individual E-cadherin/E-cadherin bonds were distributed (Fig. 5, *a* and *b*). For a given retraction velocity, the distribution of bond forces can be fitted using the Bell model (24, 27). We found excellent agreement between measured and theoretical force distributions for both parental cells and  $\alpha$ -catenin-expressing cells (Fig. 5, *a* and *b*). Because the Evans-Ritchie model assumes a single dissociation rate and a single reactive compliance, this agreement indicates that indeed one type of adhesive bonds dominates intercellular interactions between MDA468 cells and  $\alpha$ -catenin MDA468 cells (confirming results in Fig. 1*d*) and that other adhesion molecules, such as integrin and C-CAM, contribute little to intercellular adhesion at least at short contact times.

Using the recent analysis of single-molecule force spectroscopy data by Dudko *et al.* (21), we extracted the effective energy of interaction,  $E_a$ , of individual intercellular E-cadherin/E-cadherin bonds from the theoretical fits of force distributions (Fig. 5, *a* and *b*). We found that the relative depth of the energy barrier for the rupture of individual E-cadherin/E-cadherin bonds between  $\alpha$ -catenin-expressing cells was significantly deeper than for E-cadherin/E-cadherin bonds between paren-

tal cells, which lack  $\alpha$ -catenin (Fig. 5, *c* and *d*). This result indicates that intracellular protein  $\alpha$ -catenin greatly stabilizes extracellular E-cadherin/E-cadherin bonds against tensile forces. The energy profile of single intercellular E-cadherin/E-cadherin bond can be approximated by the harmonic energy potential  $E_a \approx (k_m x^2)/2$ , which defines an effective molecular stiffness  $k_m$  for the E-cadherin/E-cadherin bond and the width of the energy barrier,  $x^*$  (Figs. 5, *d* and *e*, and 6). We found that the molecular stiffness of E-cadherin intercellular bonds was much higher, and the energy barrier was much narrower and deeper in cells expressing  $\alpha$ -catenin than in parental cells lacking  $\alpha$ -catenin (Figs. 5*e* and 6). These results suggest that the conformation of individual E-cadherin/E-cadherin is significantly more rigid in cells expressing  $\alpha$ -catenin and that  $\alpha$ -catenin provides individual E-cadherin/E-cadherin bonds with additional stability against tensile forces.

To examine the potential role played by the actin cytoskeleton on E-cadherin/E-cadherin bond strength, we conducted single-molecule measurements using  $\alpha$ -catenin-expressing cells treated with F-actin-depolymerizing drug latrunculin B (concentration, 80 nM) (29). The mean bond strength was found to be only marginally decreased ( $p = 0.03$ ) compared with the same cells in the absence of latrunculin B treatment (Fig. 2*d*). This slight difference may be explained by the softening of the cytoplasm of latrunculin B-treated cells (29, 30). More importantly, the mean bond strength remained significantly higher ( $p < 0.001$ ) than the bond strength measured for  $\alpha$ -catenin null cells. The corresponding global adhesion assay for latrunculin B-treated  $\alpha$ -catenin-expressing cells reinforced the finding from our single-molecule experiments that the actin cytoskeleton does not affect the binding strength of E-cadherins between cells (Fig. 1*e*).

We further examined the influence of  $\alpha$ -catenin on E-cadherin/E-cadherin bond strength by conducting single-molecule measurements between unlike top and bottom cells. Cells expressing  $\alpha$ -catenin were plated as monolayer, and an AFM cantilever loaded with an  $\alpha$ -catenin null cell was brought in contact for a short duration ( $\sim 1$  ms). The corresponding

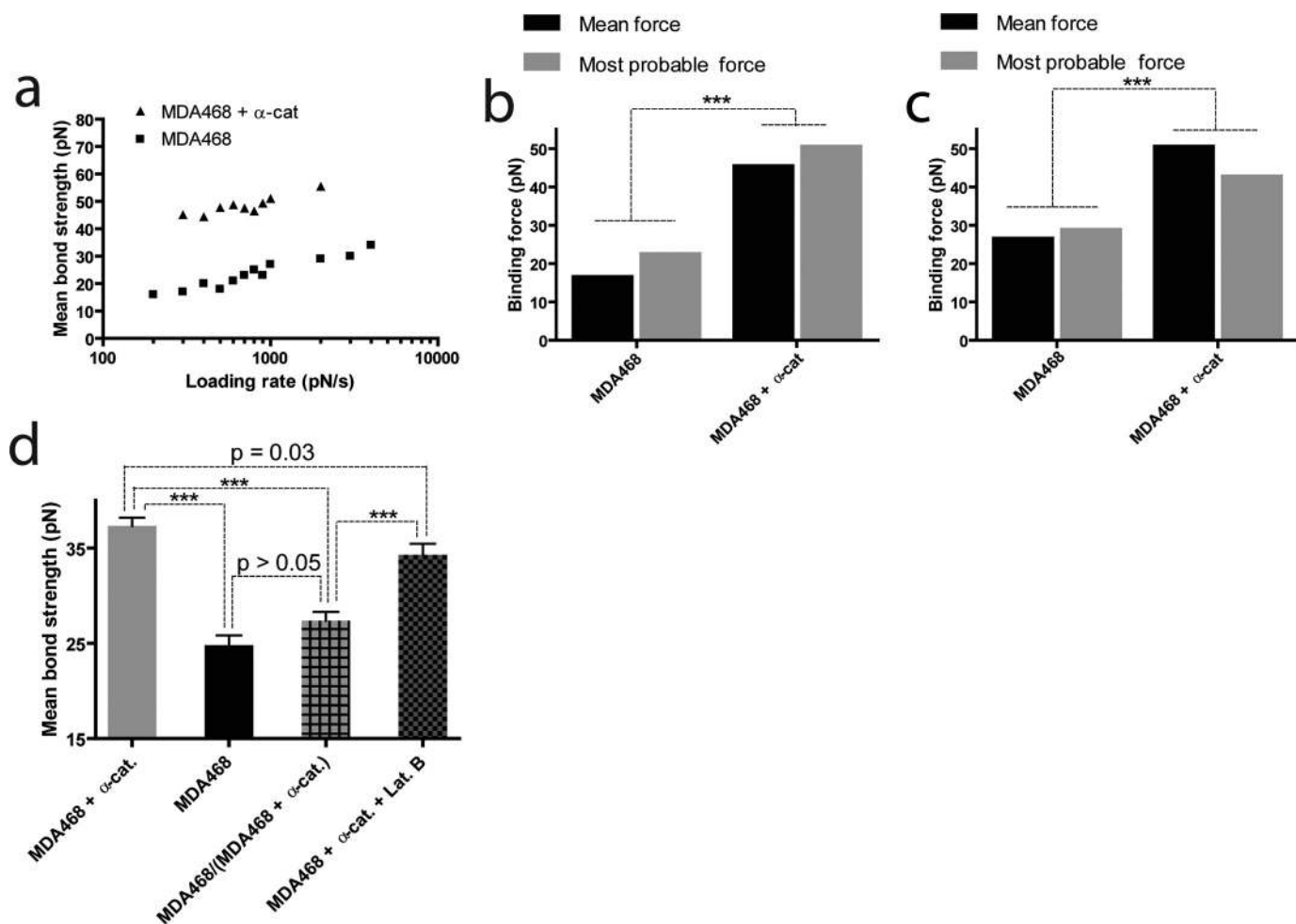


**FIGURE 3. Loss of  $\alpha$ -catenin decreases the strength of E-cadherin/E-cadherin bonds between cancer cells.** *a*, averaged tensile strength of single intercellular E-cadherin/E-cadherin bonds as a function of loading rate for MDA468 cells that lack  $\alpha$ -catenin (*lower curve*) and  $\alpha$ -catenin-expressing MDA468 cells (*top curve*). *b* and *c*, averaged and most probable bond rupture forces at binned loading rates of 300 pN/s (*b*) and 1000 pN/s (*c*) for MDA468 cells and  $\alpha$ -catenin-expressing MDA468 cells. *d*, averaged tensile strength of single intercellular E-cadherin/E-cadherin bonds between  $\alpha$ -catenin-expressing MDA468 cells (*first bar*), MDA468 cells (*second bar*), MDA468 cells and  $\alpha$ -catenin-expressing MDA468 cells (*third bar*), and  $\alpha$ -catenin-expressing MDA468 cells in the presence of latrunculin B (*fourth bar*).

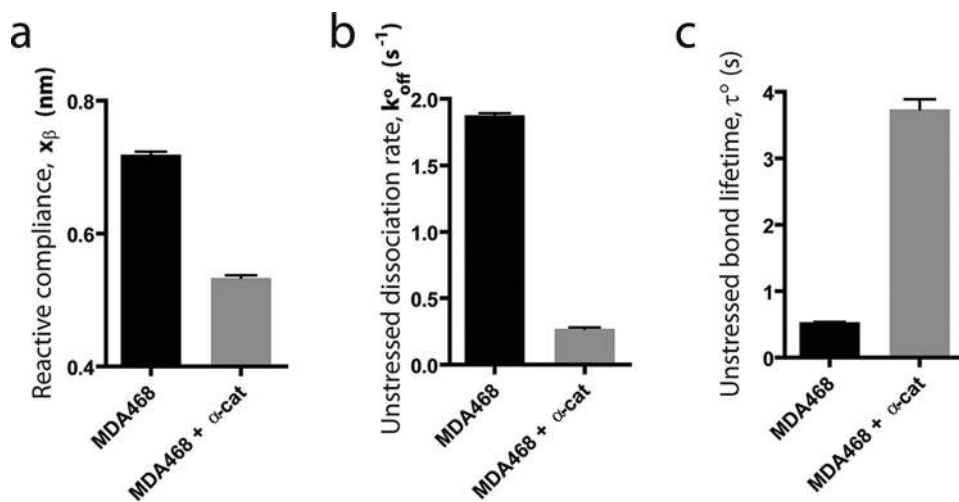


**FIGURE 4. Loss of  $\alpha$ -catenin reduces the bond lifetime and increases the reactive compliance and dissociation rate of E-cadherin intercellular bond.** Shown are the reactive compliance,  $x_\beta$  (*a*), unstressed dissociation rate,  $k_{off}^0$  (*b*), and unstressed bond lifetime,  $\tau^0 = 1/k_{off}^0$  (*c*) of individual E-cadherin/E-cadherin bonds for MDA468 cells and  $\alpha$ -catenin-expressing MDA468 cells.

mean E-cadherin/E-cadherin bond strength was closer to the strength of a bond between two  $\alpha$ -catenin null cells than the strength of a bond between two cells expressing  $\alpha$ -catenin (Fig. 3*d*). The corresponding global adhesion assay confirmed this finding (Fig. 1*e*). These results suggest that the absence of  $\alpha$ -catenin causes a dominant negative effect on both global cell-cell adhesion and E-cadherin-mediated single intercellular adhesion bond strength.

The loss of E-cadherin expression is a common feature of tumor progression and metastasis in cancers of epithelial origin (31). This is presumably because E-cadherin down-regulation reduces the global



## $\alpha$ -Catenin Enhances E-cadherin Adhesion

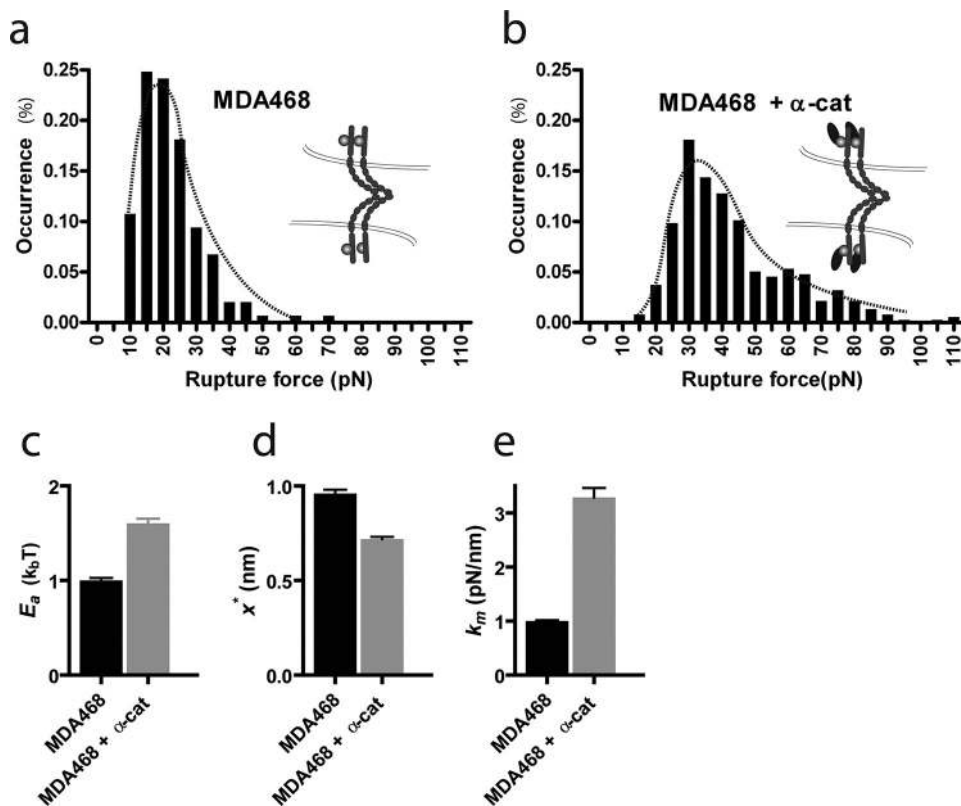


**FIGURE 5. Analysis of bond rupture force distributions.** *a* and *b*, distributions of E-cadherin/E-cadherin bond rupture forces for MDA468 cells (*a*) and  $\alpha$ -catenin-expressing MDA468 cells (*b*). Retraction velocity, 30  $\mu$ m/s. *c* and *d*, relative depth (*d*) and width (*d*) of the energy barrier for the dissociation of single E-cadherin/E-cadherin bonds between MDA468 cells (*left bars*) and between  $\alpha$ -catenin-expressing MDA468 cells (*right bars*). *e*, molecular stiffness,  $k_m$ , of single E-cadherin/E-cadherin bonds between MDA468 cells (*left bar*) and between  $\alpha$ -catenin-expressing MDA468 cells (*right bar*).

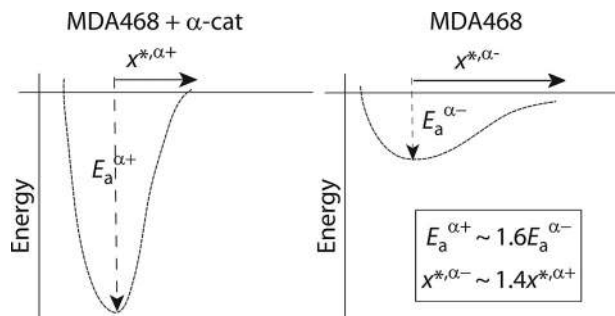


**FIGURE 6. Loss of  $\alpha$ -catenin in MDA468 human breast cancer cells causes destabilization of the E-cadherin/E-cadherin bond against tensile forces.** Schematic of the energy profiles describing E-cadherin/E-cadherin bonds between parental MDA468 cells, which lack  $\alpha$ -catenin, and MDA468 cells where  $\alpha$ -catenin was expressed.  $E_a$  is the relative depth of the energy well, and  $x^*$  is its width. The molecular stiffness of the bond is related to  $E_a$  and  $x^*$  by fitting the energy well with a harmonic potential as  $E_a \approx (k_m x^{*2})/2$ .

strength of intercellular adhesion within a tissue, therefore enhancing cellular motility (32). Re-expression of E-cadherin reduces metastatic potential of cancer cells (31, 32). However, in many types of cancers, cell detachment from a primary tumor site and transition to metastasis strongly correlates with the loss of  $\alpha$ -catenin (4–9). Moreover, the loss of  $\alpha$ -catenin seems to be sometimes a better predictor of clinical outcome than the loss of E-cadherin (5, 9). Here we show that the loss of  $\alpha$ -catenin in human breast cancer cells plays a direct and pro-

found role in reducing individual cadherin/cadherin binding interactions between adjoining cells. Specifically, the loss of  $\alpha$ -catenin drastically reduces the lifetime, tensile strength, and mechanical stability of single cadherin bonds between human breast cancer cells.

Our data suggest that the changes in bond strength are partly caused by a change in the configuration of E-cadherin/E-cadherin bonds mediated by the loss of  $\alpha$ -catenin. Indeed, the absence of  $\alpha$ -catenin in MDA468 cells reduces >3-fold the flexural rigidity of single E-cadherin/E-cadherin bonds (measured by  $k_m$ ) compared with  $\alpha$ -catenin-expressing MDA468 cells.

A mechanism that could explain the  $\alpha$ -catenin-dependent strength of individual E-cadherin/E-cadherin bonds between adjacent cells is that the presence of  $\alpha$ -catenin in the adhesion molecular-complex might induce clustering of E-cadherins caused by the dimerization of  $\alpha$ -catenins bound to adjacent E-cadherin- $\beta$ -catenin/ $\alpha$ -catenin complexes. Although our data cannot *per se* test this hypothesis directly,

we must note that such a mechanism seems improbable based on previously reported binding screen studies. Using chimeric proteins, it has been shown that the dimerization site of  $\alpha$ -catenin overlaps with its  $\beta$ -catenin-binding site (33). In other words,  $\alpha$ -catenin cannot simultaneously bind  $\beta$ -catenin and form a dimer with another  $\alpha$ -catenin bound to an adjacent E-cadherin- $\beta$ -catenin complex. Binding to  $\beta$ -catenin disrupts the dimerization of  $\alpha$ -catenin. In light of these results, it seems improbable that the observed enhanced bond strength of E-cadherin/E-cadherin bonds in  $\alpha$ -catenin-expressing cells is due to the dimerization of  $\alpha$ -catenin across the cytoplasmic domains of E-cadherin. Nevertheless, more studies need to be conducted to further test this hypothesis.

Together our results suggest the loss of intercellular adhesion commonly observed in solid tumors of epithelial origin (31, 32) may stem not only from the loss of global cell adhesion through down-regulation of E-cadherin (and ensuing reduced cadherin-mediated intercellular avidity) but also the reduction of intercellular cadherin bond strength induced by the loss of  $\alpha$ -catenin. We also show that the forced expression of  $\alpha$ -catenin in human breast cancer cells can restore both higher intercellular avidity and intercellular bond strength of E-cadherin, which suggests an alternative strategy to stop or slow down the metastatic phenotype.

**REFERENCES**

1. Guo, W., and Giancotti, F. G. (2004) *Nat. Rev. Mol. Cell Biol.* **5**, 816–826
2. Yin, T., and Green, K. J. (2004) *Semin. Cell Dev. Biol.* **15**, 665–677
3. D'Souza-Schorey, C. (2005) *Trends Cell Biol.* **15**, 19–26
4. Nakopoulou, L., Gakiopoulou-Givalou, H., Karayiannakis, A. J., Giannopoulou, I., Keramopoulos, A., Davaris, P., and Pignatelli, M. (2002) *Histopathology* **40**, 536–546
5. Kadowaki, T., Shiozaki, H., Inoue, M., Tamura, S., Oka, H., Doki, Y., Iihara, K., Matsui, S., Iwazawa, T., Nagafuchi, A., *et al.* (1994) *Cancer Res.* **54**, 291–296
6. Shiozaki, H., Iihara, K., Oka, H., Kadowaki, T., Matsui, S., Gofuku, J., Inoue, M., Nagafuchi, A., Tsukita, S., and Mori, T. (1994) *Am. J. Pathol.* **144**, 667–674
7. Yu, J., Ebert, M. P., Miehle, S., Rost, H., Lendeckel, U., Leodolter, A., Stolte, M., Bayerdörffer, E., and Malfertheiner, P. (2000) *Gut* **46**, 639–644
8. Carico, E., Atlante, M., Buccia, B., Nofroni, I., and Vecchione, A. (2001) *Gynecol. Oncol.* **80**, 156–161
9. Ropponen, K. M., Eskelinen, M. J., Lipponen, P. K., Alhava, E. M., and Kosma, V. M. (1999) *J. Clin. Pathol.* **52**, 10–16
10. Thiery, J. P., and Sleeman, J. P. (2006) *Nat. Rev. Mol. Cell Biol.* **7**, 131–142
11. Kang, Y., Siegel, P. M., Shu, W., Drobnjak, M., Kakonen, S. M., Cordon-Cardo, C., Guise, T. A., and Massagué, J. (2003) *Cancer Cell* **3**, 537–549
12. Patel, S. D., Chen, C. P., Bahna, F., Honig, B., and Shapiro, L. (2003) *Curr. Opin. Struct. Biol.* **13**, 690–698
13. Perez-Moreno, M., and Fuchs, E. (2006) *Dev. Cell* **11**, 601–612
14. Vasioukhin, V., Bauer, C., Yin, M., and Fuchs, E. (2000) *Cell* **100**, 209–219
15. Yamada, S., Pokutta, S., Drees, F., Weis, W. I., and Nelson, W. J. (2005) *Cell* **123**, 889–901
16. Bajpai, S., Correia, J., Feng, Y., Figueiredo, J., Sun, S. X., Longmore, G. D., Suriano, G., and Wirtz, D. (2008) *Proc. Natl. Acad. Sci. U.S.A.* **105**, 18331–18336
17. Dobrowsky, T. M., Panorchan, P., Konstantopoulos, K., and Wirtz, D. (2008) *Methods Cell Biol.* **89**, 411–432
18. Panorchan, P., Thompson, M. S., Davis, K. J., Tseng, Y., Konstantopoulos, K., and Wirtz, D. (2006) *J. Cell Sci.* **119**, 66–74
19. Cailleau, R., Olivé, M., and Cruciger, Q. V. (1978) *In Vitro* **14**, 911–915
20. Marie, H., Pratt, S. J., Betson, M., Epple, H., Kittler, J. T., Meek, L., Moss, S. J., Troyanovsky, S., Attwell, D., Longmore, G. D., and Braga, V. M. (2003) *J. Biol. Chem.* **278**, 1220–1228
21. Dudko, O. K., Hummer, G., and Szabo, A. (2008) *Proc. Natl. Acad. Sci. U.S.A.* **105**, 15755–15760
22. Chesla, S. E., Selvaraj, P., and Zhu, C. (1998) *Biophys. J.* **75**, 1553–1572
23. Konstantopoulos, K., Hanley, W. D., and Wirtz, D. (2003) *Curr. Biol.* **13**, R611–R613
24. Hanley, W. D., Wirtz, D., and Konstantopoulos, K. (2004) *J. Cell Sci.* **117**, 2503–2511
25. Panorchan, P., George, J. P., and Wirtz, D. (2006) *J. Mol. Biol.* **358**, 665–674
26. Ray, C., Brown, J. R., and Akhremitchev, B. B. (2007) *Langmuir* **23**, 6076–6083
27. Bell, G. I. (1978) *Science* **200**, 618–627
28. Marshall, B. T., Sarangapani, K. K., Lou, J., McEver, R. P., and Zhu, C. (2005) *Biophys. J.* **88**, 1458–1466
29. Lee, J. S., Hale, C. M., Panorchan, P., Khatau, S. B., George, J. P., Tseng, Y., Stewart, C. L., Hodzic, D., and Wirtz, D. (2007) *Biophys. J.* **93**, 2542–2552
30. Tseng, Y., Kole, T. P., and Wirtz, D. (2002) *Biophys. J.* **83**, 3162–3176
31. Cavellero, U., and Christofori, G. (2004) *Nat. Rev. Cell Mol. Biol.* **4**, 118–132
32. Mareel, M., and Leroy, A. (2003) *Physiol. Rev.* **83**, 337–376
33. Pokutta, S., and Weis, W. I. (2000) *Mol. Cell* **5**, 533–543